Environmental and Climate Technologies
2024, vol. 28, no. 1, pp. 695–711
https://doi.org/10.2478/rtuect-2024-0054
https://content.sciendo.com

Features of Heat and Mass Transfer in the Thermodynamic Equilibrium Region of Gas Hydrates

Hanna KOSHLAK[1*], Tomasz OCHRYMIUK[2]

[1]*Kielce University of Technology, aleja Tysiąclecia Państwa Polskiego, 7, 25-314, Kielce, Poland*
[2]*Institute of Fluid-Flow Machinery Polish Academy of Sciences, Fiszera 14 st. Gdańsk 80-23, Poland*

Received 20.09.2024; accepted 21.10.2024

***Abstract* – This paper presents the results of an investigation into the influence of thermodynamic parameters on diffusive hydrate formation of hydrocarbon gases. Diffusion processes at the fixed interface and intensification processes of hydrate synthesis were experimentally studied. The temperature range at which the rate of hydrate formation is maximized was determined. Additionally, a criterion for optimizing the thermodynamic parameters of the synthesis process was proposed.**

***Keywords* – Gas hydrates; phase transformations; gas pressure; gas temperature.**

Nomenclature

V_0	calculated amount of hydrate	m^3
k	rate constant of hydrate formation	s^{-1}
τ	time of hydrate formation process	s
I_H	rate of mass transfer at the interfacial surface during hydrate formation	
n	constants determined by the reaction conditions	
ΔT	supercooling in the hydrate formation region	°C
I_d	diffusive mass flux of hydrate in a fixed medium	kg m^{-2} s^{-1}
I_H	diffusive mass flux of hydrate in a mobile medium (at stirring)	kg m^{-2} s^{-1}
I	diffusive mass flux of hydrate in vapour-liquid flow (on the surface of gas bubbles)	kg m^{-2} s^{-1}
D	diffusion coefficient of gas in water	m
d	gas bubble diameter	
ρ	density of water	kg/m^3
ρ_g	density of gas	kg/m^3
R	universal gas constant	
T	water temperature	°C
T_g	gas temperature	°C
c_d	heat capacity of water	
a	thermal diffusivity	m/s^2

* Corresponding author.
E-mail address: hkoshlak@tu.kielce.pl

r	bubble radius at the current time (coordinate)	m
F_b	interface area	m^2
Δt^*	logarithmic mean temperature difference	
q_r	specific heat flux between the bubble surface and the aqueous medium	
q_g	specific heat flux from the hydrate formation surface to the gas medium of the bubble	
m	mass of hydrate	kg
β_v	volumetric mass transfer coefficient from gas to liquid,	s^{-1}
Sc	Schmidt number	
l	capillary constant	
σ	surface tension coefficient	
ε	compressibility coefficient of the gas	

1. INTRODUCTION

Gaseous hydrocarbons in contact with water at certain temperature and pressure ratios form compounds called gas hydrates (GH). Crystalline hydrates are unstable molecular compounds that decompose into their constituents, gas, and water, when the pressure is reduced or the temperature is increased.

Recent research into the properties of gas hydrates (GH) has significantly intensified due to their potential as promising sources of hydrocarbon raw materials. These hydrates, often occurring naturally and primarily composed of methane, offer a valuable alternative energy source. Estimates suggest that natural gas deposits in the form of gas hydrates could total approximately 2×10^{16} cubic meters, significantly exceeding the combined reserves of all other carbon fuels on Earth [1]–[4]. Scientific data indicate that marine sediments hold between 500 and 1000 Gt of gas hydrates, while the Arctic permafrost zone contains an estimated 400 Gt [5], [6].

At the same time, hydrates under thermobaric conditions close to dissociation are potentially environmentally hazardous. If the thermodynamic equilibrium conditions are shifted, methane can be released in free form and contribute significantly to the greenhouse effect [7], [8].

Therefore, knowledge of the dynamic, thermodynamic, and mechanical properties of gas hydrates is crucial for assessing their behaviour during the development of gas hydrate deposits.

Gas hydrates can be produced at appropriate industrial facilities. Important for their storage and transportation [9], [10] is the ability to self-preserve at temperatures below 0 degrees Celsius. That is, if the pressure over the formed hydrate is reduced, it begins to dissociate and forms a thin film of ice on its surface, which stops further decomposition. Given the high gas capacity of the hydrate (up to 164 m^3 of gas per 1 m^3 of hydrate), it is possible to store and transport the gas at atmospheric pressure in the form of solid briquettes.

The heat of decomposition of methane hydrate ($CH_4 \cdot 6H_2O$) into gas and liquid water (0 °C, 1 atm) is only 54.2 kJ/mol [3] (a value typical of supramolecular processes), while the heat of combustion of free methane is 890 kJ/mol (a value typical of chemical reactions). The decomposition of methane hydrate requires only about 6 % of the heat released by its methane combustion. Gas hydrate technologies offer several advantages, including:

- simplifying the storage and transportation of natural gases by eliminating the need for high-pressure tanks:
- increasing the efficiency of natural gas storage and transportation by reducing the dissociation pressure;
- increasing the mass content of gases per unit volume of clathrates formed, and enhancing their gas content.

The physical and chemical properties of clathrates make it possible to store and transport natural gases in conventional leaky containers using vehicles such as cars, platform wagons, and river and sea vessels. The most promising applications for gas hydrates are in the storage and transportation of natural gases. Specifically, they offer solutions for delivering and storing natural gases in remote and inaccessible residential and industrial areas. Additionally, gas hydrates can serve as generators of combustible gases for internal combustion engines, including cars and autonomous power plants. Moreover, synthesized gas hydrates enable the transportation and storage of light hydrocarbons, such as methane and ethane, which are often flared at production sites, contributing to significant environmental degradation in surrounding areas.

Natural gas is most conveniently transported and stored when it is in the form of a gas hydrate. Technologically, the formation of gas hydrates occurs when gas dissolves in water under certain thermobaric conditions. The process of gas hydrate formation takes place at the interface. There are known studies aimed at developing technology for the synthesis of gas hydrates [11], [12].

To improve the technology of GH synthesis, it is important to study the influence of various factors on this process. It is known that the rate of hydrate formation can vary widely, practically from two weeks to several minutes, and by changing the thermodynamic parameters of the synthesis, materials with predictable properties can be obtained [13]–[16].

Laboratory studies [17] show that the formation of hydrates under isochoric-isothermal conditions (static mode) takes a long time from 6 hours to several weeks. According to [3], the kinetics of methane hydrate formation is described by the equation (1).

$$V = \frac{V_0}{e^{-k\tau}}\left(e^{-k\tau} - 1\right) \tag{1}$$

A generalisation of the studies reported in [14] shows that the intensity of mass transfer during hydrate formation in a dynamic mode is represented by the following equation (2).

$$I_{\text{H}} = k \cdot \Delta T^n \tag{2}$$

Formula (2) does not contain factors such as time and pressure in the system, which, as shown by studies by other authors, significantly affect the rate of hydrate formation.

The influence of surface active substances on the hydrate formation process was investigated in [18], [19], where experimental studies showed that the surfactant concentration of up to 0.1 % reduces the hydrate formation temperature of propane by 6 °C.

The results of the study of the influence of salt concentration in water on the rate of mass transfer during hydrate formation in a chamber with an agitator are given in [20]. It was found that the rate of gas absorption decreases with increasing water salinity, and the optimal number of revolutions of the agitator impeller is 650–700 rpm.

Depending on the conditions of the process in [21]. The authors systematised five models of hydrate formation kinetics: on the surface of bubbles, hydrate film growth on the fixed surface of water, at application of stirrers, on the basis of mass transfer processes, and hydrate

crystals growth from ice. The empirical coefficients in the equations are given only for methane and ethane.

Analysis of the works of many researchers indicates insufficient information on the rate of mass exchange processes during hydrate formation. In addition, the existing literature is dominated by qualitative rather than quantitative characteristics of the influence of various means of intensification of this process. The lack of such important information significantly complicates the process of designing industrial plants for hydrate synthesis.

2. Study of Mass Transfer Processes of Hydrate Formation in the Diffusion Mode

The aim of the experiments was to determine the mass transfer rate under thermodynamic conditions of gas hydrate formation. To stabilise the temperature at a given level for a long period of time, the unit was supplemented with an external 'cold accumulator' and a thermostat, Fig. 1.

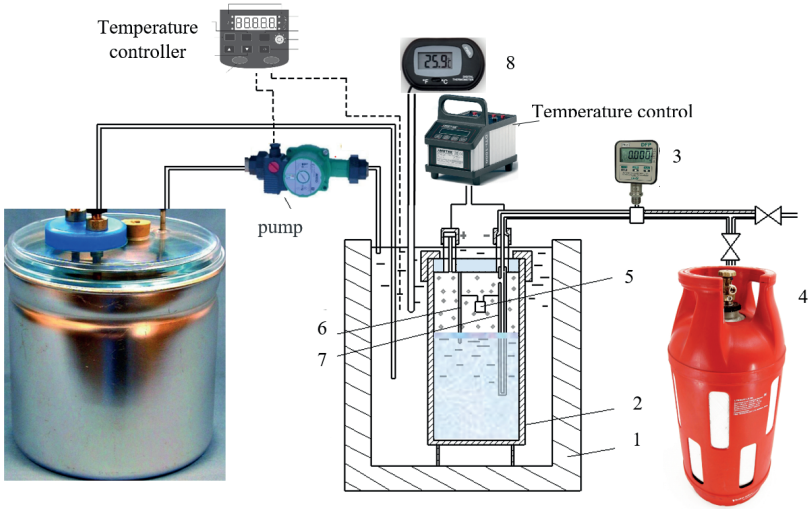

Fig. 1. Experimental installation for hydrate formation: 1 – insulated case; 2 – high-pressure vessel; 3–4 atm pressure gauge; 4 – compressed gas; 5 – electronic temperature sensor: 6, 7 – electrodes; 8 – thermometer.

In our study, we investigated the diffusive hydrate formation and its influence to highlight the main factors influencing its intensity. For this purpose, water and one of the gases (methane, propane or butane) were fed into vessel 1. A circulating thermostat AN CYRO-LTCCB was used to maintain the temperature set in vessel 1. The temperature was measured using a Pt100 thermometer. A WIKA A-10 sensor was used to measure the gas pressure.

The following methodology for the experimental studies was used. Firstly, the reactor was filled with a gas mixture at a temperature of 10–15 °C. After stabilisation of the temperature regime, the initial pressure was measured. Then the temperature in the reactor was reduced to the temperature of hydrate formation, and pressure measurement was performed. After that, the temperature in the reactor was maintained for a given time interval, and time and gas pressure were recorded. The hydrate formation process takes place at a fixed interface. The

experiment was terminated by increasing the temperature in the reactor, dissociating the hydrate, and measuring the gas volume.

To illustrate, here are some typical mass transfer characteristics for various experiments. When the temperature reaches +2.5 °C, the formation of propane hydrate begins. The pick of the formed hydrate sharply 'brakes' the process of further hydrate formation. In the region of hydrate formation, mass-exchange processes are sharply slowed down. The approximation dependence for the intensity of mass transfer during hydrate formation is of the form. This is confirmed by the experience conducted at the temperature of hydrate formation +1.8 °C (Fig. 2), where we can see how sharply decreases the mass transfer between gas and water. Approximation of the mass transfer intensity in the hydrate formation region.

$$I_d = 0.166 \cdot \tau^{-2.6} \tag{3}$$

The experiment was carried out in a temperature-stabilised unit with an external refrigerator. The temperature stabilised at +1.8 °C. A propane-butane mixture was used.

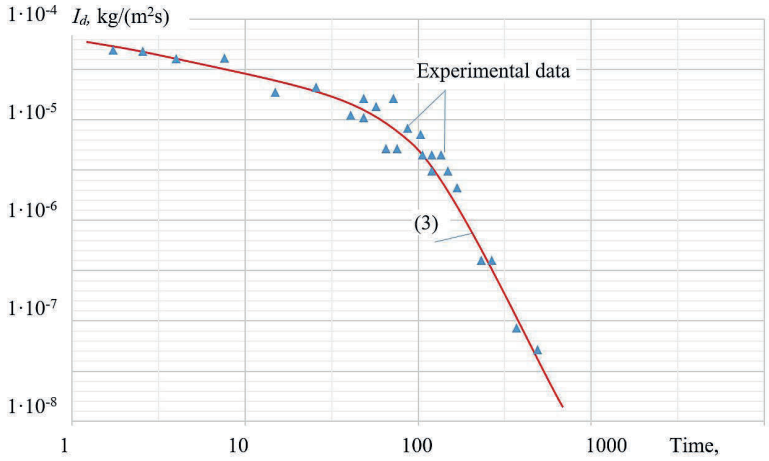

Fig. 2. Temperature and specific mass transfer under conditions of hydrate formation.

The graph shows a sharp decrease in the intensity of mass-exchange processes in thermobaric conditions of hydrate formation. However, the mass-transfer lines in the hydrate formation regime indicate the possibility of very intensive mass transfer at the initial moments of time.

2.1. Intensification of Mass Transfer Processes Using a 'Slow' Stirrer

A common means of intensifying the hydrate formation processes is mechanical destruction of the hydrate film. The simplest option for such intensification is the use of various mechanical agitators. The types of agitators can be divided into two: 'slow' agitators and 'high-speed' agitators. The speed of a slow agitator is in the range of 10–100 rpm. A high-speed agitator is characterised by frequencies of 1000–2000 rpm.

The main task of a slow stirrer is to equalise the gas concentration in the liquid and destroy the hydrate film that forms on the interfacial surface. To study the processes of intensification of mass transfer and hydrate formation, the existing pilot plant was supplemented with a mechanical stirrer (Fig. 3).

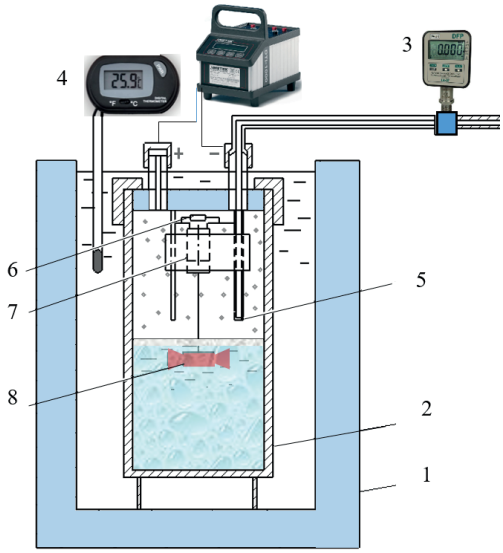

Fig. 3. Installation for research of hydrate formation processes at application of low-speed agitator with immersed impeller; 1 – heat insulated case; 2 – reactor; 3 – pressure gauge; 4 – thermometer; 5 – tubular electrode; 6 – gas temperature sensor; 7 – high-speed microelectric motor; 8 – agitator impeller.

The first series of experiments were carried out under conditions where the impeller was under the water mirror. The purpose of these experiments was to test the hypothesis of the possibility of hydrate formation from gas dissolved in water. Also, because of the underwater location of the impeller, it was planned to achieve deformation of the interfacial surface and destruction of the hydrate film. In general, the operation of the device was supposed to significantly accelerate the mass transfer processes. The results of the study of the submerged slow stirrer operation are shown in Fig. 4.

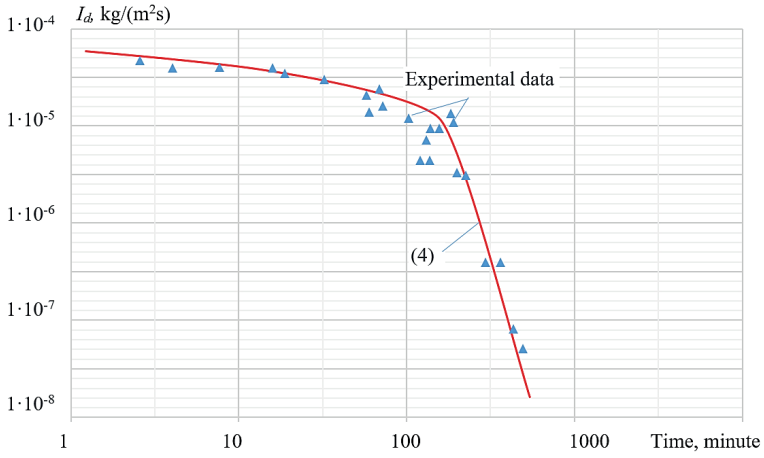

Fig. 4. Stirrer under a water mirror.

Approximation dependencies as Eq. (4).

$$I_{\mathrm{H}} = 10.7 \cdot \tau^{-3.36} \tag{4}$$

To analyse the results obtained, a comparison of the mass transfer results was performed under simple diffusion and slow stirrer conditions, Fig. 5.

It was found that the use of an agitator with 'slow' agitation and impeller located under the water mirror:

1. Leads to a significant acceleration of mass-exchange processes (up to 40 times) outside the area of hydrate formation. However, the intensification of mass transfer starts only after 10 minutes of agitation.
2. Intensification of mass transfer in the area of hydrate formation (6.4 times) is observed only after prolonged stirring (8 h).

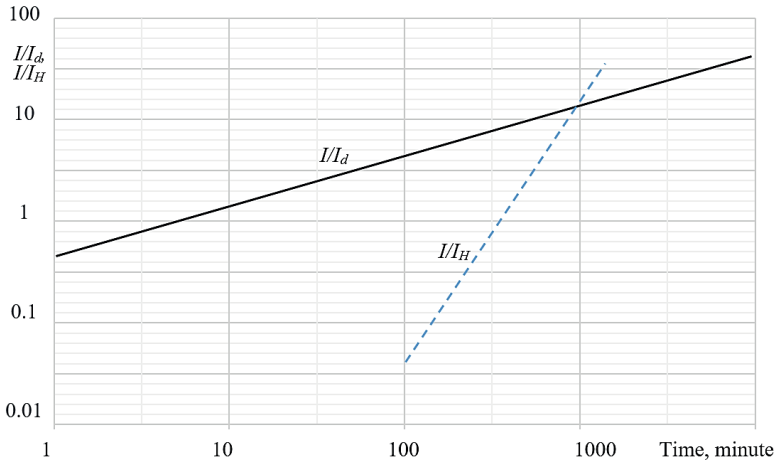

Fig. 5. Comparison of mass transfer on the gas-water surface under stationary conditions and with the use of a slow stirrer located under a water mirror.

Therefore, a relatively small effect of a slow stirrer with a 'flooded' impeller is observed on the intensification of mass transfer on the interfacial surface is observed. The heat transfer surface area does not change. Therefore, to accelerate heat and mass transfer processes at the interface and increase the heat and mass transfer area, it is necessary to intensify the mixing process.

To further intensify the mass transfer at the interfacial surface, it was decided to turbulise the interfacial surface more actively. For this purpose, the impeller of the agitator was raised to the level of the water mirror. This allows for achieving two positive results at once: permanent destruction of the hydrate film on the interfacial surface and active mixing of the liquid layers to accelerate gas diffusion into the liquid.

The stirrer impeller was mounted on the surface of the water mirror. To reduce the thermal effect of the electric motor, the studies were carried out mainly at a voltage of 1.5 V and occasionally at 3.3 V.

The results of processing the experimental data for mass transfer processes are shown in Fig. 6.

On the basis of the statistical processing of the experimental data, the following dependence was obtained as in Eq. (5).

$$I_{\text{H}} = 0.02 \cdot \tau^{-1.62} \tag{5}$$

To compare the performance of the two types of agitators under the same conditions, the approximation lines are plotted on one diagram, Fig. 6.

The analysis of the dependencies obtained shows that:

1. The surface stirrer activates mass transfer at the beginning of the process.
2. The surface stirrer significantly accelerates mass transfer processes in the area of hydrate formation.

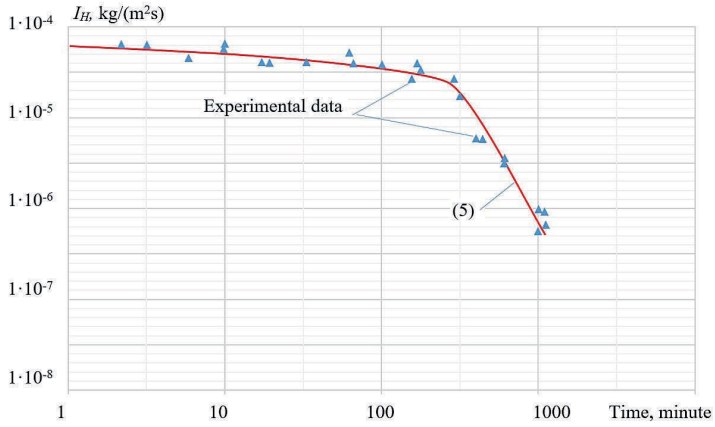

Fig. 6. Experimental data and their approximation.

The use of mechanical stirrers accelerates the mass transfer processes at the interface by 10 and more times. This effect is manifested at long stirring and increases with the increase of stirrer speed. The stirrer with a buried impeller in the time interval from 1 to 10 minutes gives somewhat worse results, due to the need to 'accelerate' the total mass of water in the reactor.

In Fig. 7 shows approximation curves for mass-exchange processes in the area of hydrate formation.

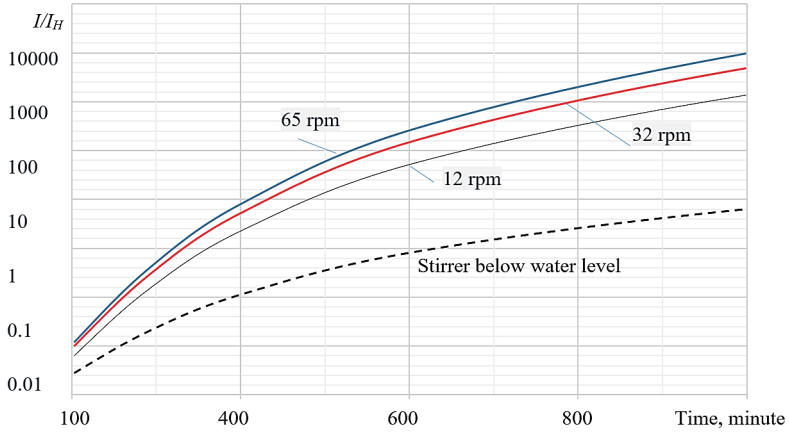

Fig. 7. Mass transfer within the hydrate formation region when using stirrers with different impeller speeds in comparison with the diffusion mode in a stationary medium

The analysis of experimental studies shows that in the field of hydrate formation at the initial moment of time, the use of mechanical stirrers slows down mass transfer, especially for a stirrer with a flooded impeller. This phenomenon occurs because at the beginning of the hydrate formation process, mass transfer processes are intense, and heat from the stirrer motors negatively affects this process. The intensity of mass transfer for surface stirrers is much higher than that for submerged stirrers. Increasing the number of revolutions and, consequently, the power of the electric motor worsens mass transfer during hydrate formation. In our opinion, this is due to the introduction of additional heat from the electric motor. The advantages of agitators over natural convection are apparent only during prolonged stirring.

Over time, the intensity of mass transfer in a stationary medium decreases rapidly, and then the use of slow mechanical stirrers begins to justify itself. A submersible stirrer is the least conducive to increasing mass transfer. The best results were obtained with a surface stirrer at 14.5 rpm. At higher speeds, the heat input from the electric motor increases 3.5 times and 10.7 times, respectively. Therefore, with an increase in the speed of the stirrer impeller, we observe slightly worse indicators of mass transfer intensification. Thus, the results obtained show the possibility of using slow stirrers to intensify mass transfer, but it is desirable to use a magnetic clutch to transfer force from the electric motor to the stirrer impeller.

The analysis of the results shows that the use of a slow surface stirrer allows for the activation of the diffusion process and the process of hydrate formation. The surface stirrer activates the diffusion process, even at low rotational speeds. In the area of hydrate formation, it does not help to accelerate the hydrate formation process Mass transfer is still significantly slowed down.

The main problem with slow agitators is the small mass-transfer surface area. Therefore, further studies were performed using a high-speed stirrer.

2.2. Intensification of Mass Transfer Processes Using a High-Speed Stirrer

An additional increase in the mass transfer surface area was achieved by using a ‘high-speed’ stirrer. Also, the pilot plant was supplemented with means of accurate measurement of gas volume and means of modelling various technological processes of gas hydrate production.

The scheme of the installation with a high-speed stirrer is shown in Fig. 8. The number of revolutions in water is 1500 rpm.

The peculiarity of the work of such an agitator is the formation of a vortex during the rotation of the impeller. This vortex draws gas inside, the agitator blades break the continuous gas flow into separate bubbles, which are picked up by the water flow and carried first to the lower part of the reactor, and then under the walls, rise to the water surface and burst.

This agitator dramatically increases the number of bubbles of different sizes. As a consequence, the surface area of the phase contact increases, and the speed of mass and heat exchange processes increases significantly. The disadvantage of the speed stirrer operation is the additional heat input from the electric motor, which heats the gas in the reactor. Therefore, during the experiments, the high-speed stirrer was only briefly for 10–20 seconds. The peculiarity of the work of such a screw at speeds of 1500 rpm is the formation of a whirlpool in which the gas is sucked in, then it is crushed into a large number of bubbles, which rotate around the screw and gradually rise to the surface of the liquid, Fig. 8b.

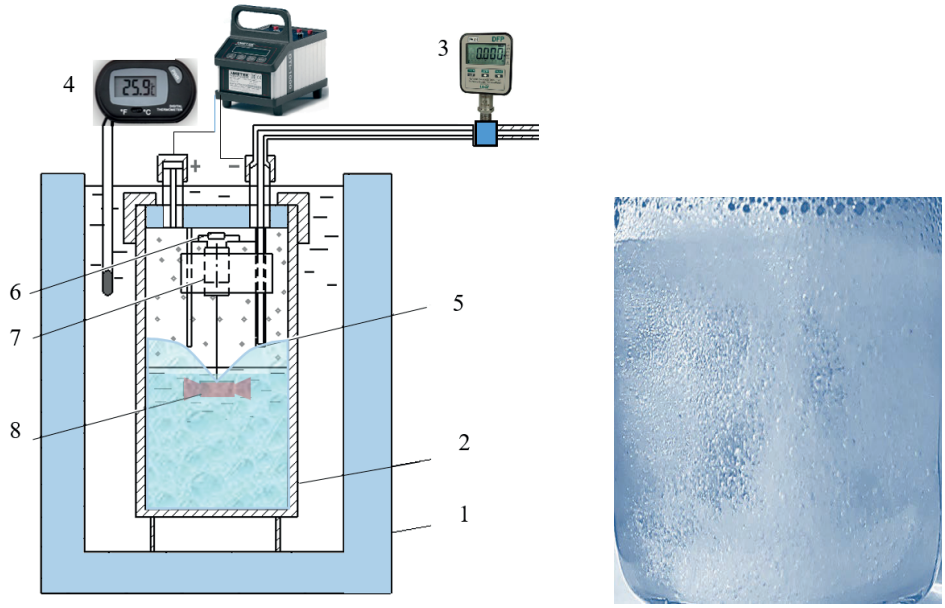

Fig. 8. Installation for hydrate formation research at application of high-speed stirrer: a) designation as in Fig. 3; b) flow structure.

The operation of the high-speed stirrer is characterised by a sharp increase in the effective area of the heat and mass exchange surface due to the formation of a large number of gas bubbles with sizes of 1–3 mm. The experiments were carried out at operation of the refrigeration unit with thermostat. The temperature of water and gas was stabilised at a given level within 0–2 °C. The components of the investigated mixture: propane and distilled water. The measurements results show that during the operation of the stirrer motor the volumetric heat gain reaches 10.1 W/L. Due to this, there is an increase of the gas temperature in the reactor by 0.6–1.4 °C. Therefore, during the experiments, the high-speed stirrer was switched on only briefly, for 12–20 s.

Analysis of the measurement results (Fig. 9) shows a significant activation of mass transfer. Approximation formula to determine the increase in the intensity of mass transfer outside the hydrate formation zone compared to the free diffusion mode (R^2 = 0.88):

$$I = I_{\mathrm{d}} \left\{ 1 + 24 \cdot e^{-3.18\tau} \right\}, \tag{6}$$

where τ is time, hour. Experimental data show activation of mass transfer by 12–13 times, and approximation dependence predicts the possibility of activation by 25 times. However, already after 40 minutes after the beginning of mass transfer, the application of high-speed agitator becomes ineffective.

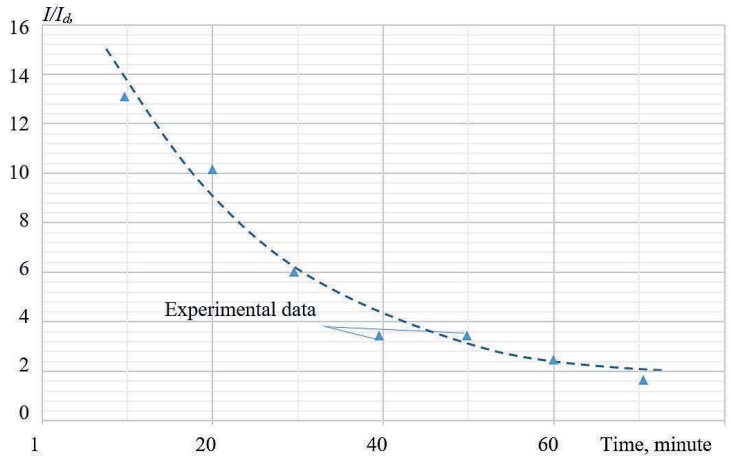

Fig. 9. Increase in the intensity of mass transfer between propane and water upon application of high-speed stirrer, in comparison with the mode of free diffusion.

Approximation formula to determine the relative intensification of mass transfer under hydrate formation conditions ($R^2 = 0.89$):

$$I = I_{\mathrm{d}} \left\{ 1 + 14.7 \cdot e^{-1.53\tau} \right\}, \tag{7}$$

where τ is time, h.

Thus, the operation of the high-speed stirrer is able to activate mass transfer 7–8 times at the beginning of the hydrate formation process, which can have a positive effect on the technology of gas hydrate synthesis. Obviously, the main means of mass transfer intensification are gas bubbles.

3. Heat Exchange Processes at the Interfacial Surface

An important condition for the formation of gas hydrate is the active process of heat removal from the reaction region. Since the main mass transfer processes take place on the bubble surface, the following ways of its cooling can be outlined:

- cooling of the water within the reactor, which is organised by supplying cooling liquid. This method is characterised by simplicity of application, low cost, and low efficiency, especially for apparatuses of large size;
- cooling of water outside the reactor. This method requires the use of additional heat exchange equipment, which complicates the design. It is characterised by the possibility of freezing of cooling surfaces of the heat exchanger and the possibility of creating small-sized bubbles in jet-type apparatuses;
- reduction of gas temperature due to the Joule-Thompson effect. It is achieved by throttling the gas before its contact with water. It is characterised by simplicity of execution, low cost, and possibility of nozzle freezing at large pressure drops. The overwhelming number of gas bubbles has large dimensions;
- reduction of gas temperature in the bubble by vaporisation of liquid components of the gas mixture. This method is characterised by high efficiency of heat removal from the interfacial surface, large bubbles, and can only be used for gases that liquefy at temperatures above 273 K.

In the existing literature, the issues of heat transfer between the internal medium and the reactor wall are most widely covered [22]. Based on numerous studies in [23], [24], it was concluded that the heat transfer coefficient does not depend on the properties of the gas, the pressure in the apparatus (up to 2 MPa), the surface tension, the gas distributor design, and the direction of the heat flow.

The heat transfer coefficient is significantly influenced by the reduced velocity of the bubbling gas vg and fluid properties (viscosity, thermal conductivity). Thermal resistance is limited by heat transfer in the liquid wall zone. To calculate the heat transfer coefficient in bubbling liquid layers with viscosity up to 0.1 Pa s, average gas capacity $\varepsilon_g \leq 0.3$ and with $K_b \leq 18$, we can apply the criterion Eq. (8) [15]:

$$\mathrm{Nu}^* = 0.43 + 0.583\mathrm{Re}^{0.471}\mathrm{Pr}^{0.31}, \tag{8}$$

where Re is the Reynolds criterion.

For several characteristic diameters of propane bubbles in water, the calculation results are summarised in Table 1.

TABLE 1. VALUES OF DIMENSIONLESS NUMBERS FOR A GAS BUBBLE

Calculated values	**Bubble diameter, mm**			
	1	**5**	**10**	**15**
Bubble rise velocity, m/s	0.1	0.22	0.25	0.28
Reynolds criterion, Re	56	615	1397	2346
Prandtl criterion, Pr	12.98	12.98	12.98	12.98
Nusselt criterion, Nu	9.02	27.0	39.5	50.3
Heat transfer coefficient, α	15 040	8999	6588	5594
Bubble heating time, s	$1.22 \cdot 10^{-4}$	$1.02 \cdot 10^{-3}$	$2.78 \cdot 10^{-3}$	$4.91 \cdot 10^{-3}$
Bubble displacement, mm	0.0122	0.2240	0.6953	1.3758

From the data in the table it can be seen that the heat exchange processes on the outer surface of the bubble are very intensive.

The basis of the heat exchange between the gaseous medium of the bubble and its interfacial surface is the diffuse mass flow described by the equation, kg m^{-2} s^{-1}:

$$I_d = \frac{4D}{d}\left(\rho - \rho_g\right). \tag{9}$$

Based on the temperature difference, the density difference can be estimated using the formula, kg/m^3:

$$\rho - \rho_g = \frac{P\mu}{RTT_g}\left[T - T_g\right]. \tag{10}$$

Heat flux transferred with the diffusing gas:

$$Q_d = \pi d^2 I_d c_d \left[T - T_g\right]. \tag{11}$$

The calculation results are summarised in Table 2.

TABLE 2. CALCULATION PARAMETERS

Calculated values	Bubble diameter, mm			
	1	**5**	**10**	**15**
Molecular diffusion coefficient, m^2/s (T = 273 K, P = 0.3 MPa)	$3.26 \cdot 10^{-6}$	$3.26 \cdot 10^{-6}$	$3.26 \cdot 10^{-6}$	$3.26 \cdot 10^{-6}$
Density difference at 10 °C temperature difference, kg/m^3	0.206	0.206	0.206	0.206
Diffusion mass flux, $kg/(m^2 \cdot s)$	26.8	5.35	2.68	1.78
Bubble heating time, s	$3.67 \cdot 10^{-5}$	$9.18 \cdot 10^{-4}$	$3.67 \cdot 10^{-3}$	$8.27 \cdot 10^{-3}$
Bubble displacement, mm	0.0037	0.202	0.919	2.315

The calculation results (Table 2) show that the heat transfer on the inner surface of the bubble is also very intensive, especially for bubbles of small size.

Normally, the heat transfer process inside the gas medium of the bubble will consist of heat transfer by gas conduction and convective flows. For bubbles up to 15 mm in size, the influence of convection can be neglected. Then, the process of heat transfer by heat conduction inside the bubble is defined by the formula (12):

$$\frac{\partial t}{\partial \tau} = a\left\{\frac{\partial^2 t}{\partial r^2} + \frac{2\partial t}{r\partial r}\right\}, \tag{12}$$

where a is the thermal conductivity of the gas, m/s. Under the following initial and boundary conditions:

$$\begin{cases} t(r,0) = t_0; \\ t(R,\tau) = t_r; \\ \dfrac{\partial t}{\partial r}(0,\tau) = 0. \end{cases} \tag{13}$$

From the solution of Eq. (12)–Eq. (13) for cooling the gas in the bubble, it follows that the heat transfer process is almost complete when the Fourier criterion $Fo \geq 0.4$. Thus, it is possible to determine the time after which the gas inside the bubble is completely heated, s:

$$\tau = \frac{Fo\,R^2}{a}. \tag{14}$$

The results of the calculation of the thermal conductivity of the bubble gas are shown in Table 3.

TABLE 3. CALCULATION PARAMETERS

Calculated values	Bubble diameter, mm			
	1	**5**	**10**	**15**
Bubble rise velocity, m/s	0.1	0.22	0.25	0.28
Thermal diffusivity of propane, m/s^2 (T = 273 K, P = 0.3 MPa)	$1.44 \cdot 10^{-6}$	$1.44 \cdot 10^{-6}$	$1.44 \cdot 10^{-6}$	$1.44 \cdot 10^{-6}$
Bubble heating time, s	0.07	1.74	6.94	15.63
Bubble displacement, mm	6.94	382	1736	4375

Thus, the process of heating the bubble due to the thermal conductivity of the gas is the slowest. If the height of the liquid layer is lower than that required to complete the transient processes, the residual average temperature difference can be determined by the formula (15):

$$\Delta t = \Delta t_0 \sum_{n=1}^{\infty} \frac{6}{n^2 \pi^2} e^{-n^2 \pi^2 Fo} . \tag{15}$$

To determine the amount of heat removed from the area of hydrate formation, we draw up a heat balance. Specific heat fluxes at the bubble surface, W/m^2:

$$q = q_{\text{r}} + q_{\text{g}} , \tag{16}$$

where q_{r} is the specific heat flux between the bubble surface and the aqueous medium; q_{g} is the specific heat flux from the hydrate formation surface to the gas medium of the bubble.
The components of heat fluxes can be revealed through the known formulas, W/m^2:

$$q = \frac{rm}{F_{\text{b}} \tau} , \tag{17}$$

$$q_{\text{g}} = \alpha_{\text{r}} \left(T - T_{\text{g}} \right), \tag{18}$$

$$q_{\text{r}} = \frac{m c_{\text{g}} \Delta t^*}{F_{\text{b}}} , \tag{19}$$

where Δt^* is the logarithmic mean temperature difference.

Substitute the heat flux values into (17) and determine the mass of the hydrate formed:

$$m = \frac{F_{\text{b}} \tau}{r} \left\{ \alpha_{\text{r}} \left(T - T_{\text{g}} \right) + \frac{m c_{\text{g}} \Delta t^*}{F_{\text{b}}} \right\} . \tag{20}$$

Thus, in the case of heat transfer between a gas in a bubble and water, the slowest heat transfer process is the heat conduction of the gas inside the bubble. It is this process that limits the heat transfer between the bubble and the liquid.

4. Mass Transfer Processes in the Interfacial Surface

Hydrate formation is based not only on thermal but also on mass transfer processes. Each of them, under certain conditions, can limit the reaction rate. However, with a 'good' ratio of thermal and mass transfer processes, hydrate can be produced quickly and of high quality.

Numerous experimental data on gas-to-liquid mass transfer in void barbotage apparatuses are summarised in [25]–[27] by an empirical criterion equation (21):

$$\frac{\beta_{\text{v}} l^2}{D} = 0.05 \text{ReSc}^{0.5} = 0.05 \frac{v_{\text{g}} l}{v_{\text{r}}} \left(\frac{v_{\text{r}}}{D} \right)^{0.5} , \tag{21}$$

where β_{v} – volumetric mass transfer coefficient from gas to liquid, s^{-1}; $\beta_{\text{v}} = \beta_{\text{F}} \cdot S_{\text{v}}$; Sc – Schmidt number; l – capillary constant; D – molecular diffusion coefficient of gas to liquid. Capillary constant:

$$l = \left(\frac{\sigma}{\rho g} \right)^{0.5}. \tag{22}$$

Surface mass transfer coefficient from gas to liquid with energy dissipation rate E in the liquid:

$$\beta_v = 0.24 \left(D \left(\frac{E}{V} \right)^{0.5} \right)^{0.5}. \tag{23}$$

According to the law of convective diffusion, the amount of gas transferred to the water surface:

$$m_g = \beta_v \cdot cF\tau. \tag{24}$$

To optimise the synthesis of gas hydrates, it is necessary to coordinate the heat and mass transfer processes at the interfacial surface. For this purpose, we propose applying the optimisation criterion, which can be obtained by considering the system of equations of heat and mass transfer on the interfacial surface, W/m^2 and kg/(s·m^2):

$$\begin{cases} \Delta m = \beta_v \left(\rho - \rho_g \right) \\ q = \alpha \left(T - T_g \right) \\ q = \dfrac{\Delta m r}{F_b} \end{cases}. \tag{25}$$

Substituting from the system of Eq. (25) gives the ratio, (°C·m^3)/kg:

$$\frac{\left(T_g - T \right)}{\left(\rho - \rho_g \right)} = \frac{\beta_v r}{\alpha m_g}. \tag{26}$$

Applying the Nusselt criteria for heat transfer Nu and diffusion Nu_d, the right part of Eq. (26) can be rewritten as follows:

$$\frac{\beta_v r}{\alpha m_g} = \frac{Nu_d}{Nu} \frac{Dr}{\lambda m_g}, \tag{27}$$

where the ratio of the Nusselt criteria and is an optimisation criterion for gas hydrate synthesis:

$$\Psi = \frac{Nu_d}{Nu}. \tag{28}$$

If we take into account the above equations, we obtain the value of the optimisation criterion as follows:

$$\Psi = \frac{\lambda m_g R \varepsilon T T_g}{DP\mu r}, \tag{29}$$

where ε is the compressibility coefficient of the gas.

This provides a criterion for optimising the heat- and mass-exchange processes in the synthesis of gas hydrates at the interface, which can be applied to the design of the synthesis apparatus.

5. CONCLUSION

Hydrate formation processes by diffusion are very slow, but can be significantly accelerated by using diffusive-convective mechanisms of heat and mass transfer.

To intensify the technology of hydrate synthesis, the application of low-speed stirrers with the location of the impeller under the water mirror is considered. Compared to free diffusion through an indestructible interface, activation by mechanical stirrers accelerates mass-exchange processes at the interface dozens of times. However, this effect manifests itself only with long stirring (more than 12 hours). The location of the impeller of the agitator on the interface surface allows intensifying mass exchange processes 2–3 times compared to the deep location. However, at values of thermodynamic parameters corresponding to the area of hydrate formation, the mass exchange is still significantly slowed down and the increased voltage of the motor leads to an increase in the heat inputs and gas heating inside the reactor.

Compared to the free diffusion mode, the use of high-speed stirrer allows one to increase the intensity of mass transfer about 7–8 times, but this effect is observed only during the first two hours. The results of the study indicate that the mass transfer intensification effect is achieved by increasing the interfacial surface area with the formation of a large number of gas bubbles. The measurements showed that immediately after switching off the high-speed stirrer, there is a sharp decrease in the mass transfer intensity. The reason for this is the decrease in the number of bubbles after the stirrer.

Thus, the most significant effect of activation of diffusion processes in hydrate formation is the presence of gas bubbles, on the surface of which water crystallises and hydrate is created. Constant deformation of the bubble shape favours the destruction of the hydrate crust, and a new hydrate layer is immediately formed on the free surface. This paper analyses the influence of heat and mass transfer processes and thermodynamic parameters on this process and proposes a criterion for optimising these parameters, which may be useful for designing gas hydrate synthesis technologies.

REFERENCES

[1] Lallouche A., Kolodyaznaya V., Boulkrane M. S., Baranenko D. Low Temperature Refrigeration as an Alternative Anti-Pest Treatment of Alexei, V. Milkov Global estimates of hydrate-bound gas in marine sediments: How much is really out there? *Earth-Sci. Rev*. 2004:66:183–197. https://doi.org/10.1016/j.earscirev.2003.11.002

[2] Boswell R., Collett T. S. Current perspectives on gas hydrate resources. *Energy Environ. Sci*. 2011:4:1045–1528. https://doi.org/10.1039/C0EE00203H

[3] Pavlenko A. M. Thermodynamic Features of the Intensive Formation of Hydrocarbon Hydrates. *Energies* 2020:13(13):3396. https://doi.org/10.3390/en13133396

[4] Pavlenko A. M., Koshlak H. A New Method for the Rapid Synthesis of Gas Hydrates for their Storage and Transportation. *Environmental and Climate Technologies* 2022:26(1):199–212. https://doi.org/10.2478/rtuect-2022-0016

[5] Brown T. D., Taylor C. E., Bernardo M. P. Rapid Gas Hydrate Formation Processes: Will They Work? *Energies* 2010:3:1154–1175. https://doi.org/10.3390/en3061154

[6] Chong Z. R., Yang S. H., Babu P., Linga P., Li X. S. Review of natural gas hydrates as an energy resource: Prospects and challenges. *Applied Energy* 2016:162:1633–1652. https://doi.org/10.1016/j.apenergy.2014.12.061

[7] Pavlenko A. M. Self-preservation Effect of Gas Hydrates. *Roc. Och. Srod*. 2021:23:346–355. https://doi.org/10.54740/ros.2021.023

[8] Pavlenko A. M. Energy conversion in heat and mass transfer processes in boiling emulsions. *Therm. Scien. Eng. Prog.* 2019:15:100439. https://doi.org/10.1016/j.tsep.2019.100439

[9] Andersson V., Kvlrner A., Norway O., Haines M. Gas hydrates for deep ocean storage of CO_2 - Novel technology for utilising hydrates for transport of CO_2. Proceedings of the 7th International Conference on Greenhouse Gas Control Technologies. 5 September 2004, Vancouver, Canada, 2005. https://doi.org/10.1016/B978-008044704-9/50169-5

[10] Takeya S., Ebinuma T., Uchida T., Nagao J., Narita H. Self-preservation effect and dissociation rates of CH4 hydrate. *J. Crystal Growth* 2002:237–239:379–382. https://doi.org/10.1016/S0022-0248(01)01946-7

[11] Pavlenko A. Application of Synthesized Hydrates in the National Economy. *Environmental and Climate Technologies* 2024:28(1):149–164. https://doi.org/10.2478/rtuect-2024-0013

[12] Pavlenko A., Koshlak H. Intensification of Gas Hydrate Formation Processes by Renewal of Interfacial Area between Phases. *Energies* 2021:14:5912. https://doi.org/10.3390/en14185912

[13] Basok B., Davydenko B., Pavlenko A. M. Numerical Network Modeling of Heat and Moisture Transfer through Capillary-Porous Building Materials. *Materials* 2021:14(8):1819. https://doi.org/10.3390/ma14081819

[14] Koshlak H., Pavlenko A. Method of formation of thermophysical properties of porous materials. *Roc. Och.Srod*. 2019:21(2):1253–1262.

[15] Pavlenko A. M. Energy conversion in heat and mass transfer processes in boiling emulsions. *Therm. Scien. Eng. Prog.* 2019:15:100439. https://doi.org/10.1016/j.tsep.2019.100439

[16] Pavlenko A., Koshlak H. Production of porous material with projected thermophysical characteristics. *Metal. Min.Ind.* 2015:7(1):123–127.

[17] Pavlenko A. Self-preservation Effect of Gas Hydrates. *Rocznik Ochrona Środowiska* 2021:23:346–355. https://doi.org/10.54740/ros.2021.023

[18] Filarsky F., Schmuck C., Schultz H. J. Development of a Surface-Active Coating for Promoted Gas Hydrate Formation. *Chem. Ing. Tech*. 2019:91(12):85–91. https://doi.org/10.3390/molecules26123615

[19] Cheng C., Wang F., Tian Y., Wu X., Zheng J., Zhang J., Li L., Yang P., Zhao J. Review and prospects of hydrate cold storage technology. *Renew. Sustain. Energy Rev*. 2020:117:109492. https://doi.org/10.1016/j.rser.2019.109492

[20] Veluswamy H. P., Kumar A., Kumar R., Linga P. An innovative approach to enhance methane hydrate formation kinetics with leucine for energy storage application. *Applied Energy* 2017:188:190–199. https://doi.org/10.1016/j.apenergy.2016.12.002

[21] Veluswamy H. P., Kumar A., Seo Y., Lee J. D., Linga P. A review of solidified natural gas (SNG) technology for gas storage via clathrate hydrates. *Applied Energy* 2018:216:262–285. https://doi.org/10.1016/j.apenergy.2018.02.059

[22] Wang C., Li X., Liang S., Li Q., Pang W., Zhao B., Chen G., Sun C. Modeling on effective thermal conductivity of hydrate-bearing sediments considering the shape of sediment particle. *Energy* 2023:285:129338. https://doi.org/10.1016/j.energy.2023.129338

[23] Majid A. A. A., Koh C. A. 8 – Self-preservation phenomenon in gas hydrates and its application for energy storage, Elliot R. Bernstein (Eds.). In *Developments in Physical & Theoretical Chemistry, Intra- and Intermolecular Interactions Between Non-covalently Bonded Species* 2021:267–285. https://doi.org/10.1016/B978-0-12-817586-6.00008-6

[24] Zhao J., Lv Q., Li Y., Yang M., Liu W., Yao L., Wang S., Zhang Y., Song Y. In-situ visual observation for the formation and dissociation of methane hydrates in porous media by magnetic resonance imaging. *Magn. Reson. Imaging* 2015:33(4):485–490. https://doi.org/10.1016/j.mri.2014.12.010

[25] Zhang P., Chen X., Li S., Wu Q., Xu Zh. Heat transfer and water migration rules during formation/dissociation of methane hydrate under temperature fields with gradient. *International Journal of Heat and Mass Transfer* 2021:169:120929. https://doi.org/10.1016/j.ijheatmasstransfer.2021.120929

[26] Kiran B. S., Sowjanya K., Prasad P. S., Yoon J. H. Experimental investigations on tetrahydrofuran-methanewater system: Rapid methane gas storage in hydrates. *Oil & Gas Science and Technology. Rev. IFP Energies Nouvelles* 2019:74:12. https://doi.org/10.2516/ogst/2018092

[27] Siažik J., Malcho M. Accumulation of primary energy into natural gas hydrates. *Procedia Eng*. 2017:192:782–787. https://doi.org/10.1016/j.proeng.2017.06.135